The Cationic Halochromism of Phenolate Betaines: Molecular Dynamics and Quantum Mechanics Studies

M. Domínguez and M. Caroli Rezende*

Facultad de Química y Biología, Universidad de Santiago, Casilla 40, Correo 33, Santiago, Chile

The cationic halochromism of phenolate betaines was reproduced with the aid of a simple theoretical model, by calculation of the longest wavelength transition energies of supermolecules obtained by positioning a cation M^{n+} at a variable distance from the oxygen atom of the dye. The theoretical results were compared with experimental data for three systems, Reichardt's betaine **1**, Brooker's merocyanine **2** and the N-methyl-8-oxyquinolinium dye **3**. The model was validated by molecular dynamics simulations of solutions of dye **3**, in methanol and DMSO, in the presence of variable concentrations of Na^+.

INTRODUCTION

The term halochromism is employed with two different, though related, meanings. It may designate the spectral behaviour of compounds in solution whose absorptions are pH-dependent [1], or of compounds which exhibit substantial changes in their UV-Vis spectra by the addition of salts [1-4].

We have been interested for some time in the study of the latter type of halochromism, and have distinguished a cationic and an anionic halochromism [5], depending on the nature of the added species responsible for the halochromic shifts in solution. Examples of cationic halochromism are found in solutions of solvatochromic phenolate dyes [6-8]. For example, addition of increased concentrations of alkaline or alkaline-earth perchlorates to alcoholic solutions of Reichardt's $E_T(30)$ betaine leads to significant colour changes, and hypsochromic shifts of its solvatochromic charge-transfer band [6], as a result of ion-pair formation between the cation and the phenolate donor moiety [7,8]. This ion-pair association

―――――――

*Corresponding author. E-mail: marcos.caroli@usach.cl

depends on the solvent, increasing sharply in alcohols of relatively low polarity.

Since the position of the charge-transfer band of the $E_T(30)$ betaine is used as a measure of the polarity of the medium, we may ascribe a "polarity value" to alcoholic electrolyte solutions of variable concentrations [6]. Alternatively, we may regard these systems as binary mixtures with polarity values that depend on the concentration of the cationic "co-solvent" [9].

The cationic halochromism of phenolates like the $E_T(30)$ betaine has been assumed to be due to the dye-cation equilibria in solution [10]. Plots of the charge-transfer-band λ_{max} value of the dye against the concentration of the added cation yield titration curves which reflect shifts in the equilibrium between the free and the cation-bound dye in solution. This picture implicitly assumes the presence of two different species in solution, the free phenolate betaine and the intimate phenolate-cation pair.

In an alternative view, we may postulate, for a given cation concentration, the existence of only one solvent-separated phenolate-cation pair, in which the average phenolate-cation

separation depends on the concentration of the added cation. According to this model, the gradual addition of a cation to the phenolate solution affects the charge-transfer transition-energy of the betaine by generating increasingly tighter phenolate-cation pairs, whose spectral response tends to the limit situation of an intimate pair.

Such a model should find support in molecular dynamics simulations of solvatochromic phenolates in solution, in the presence of variable concentrations of an added cation. As far as we know, no attempts have been made to apply molecular dynamics simulations to the interpretation of the cationic halochromism of phenolate betaines in solution.

Following this protocol, we simulated methanol and DMSO solutions of a solvatochromic betaine in the presence of variable concentrations of Na^+. The radial distribution of the sodium cations in the betaine solvating shell was used as a picture of the solvent-separated phenolate-cation pairs in these solutions. Such picture validated a simple model for the cationic halochromism of different betaines. This model was based on the calculation of the transition-energy of the longest-wavelength band of the dye in the presence of a cation positioned at a variable distance from its phenolate oxygen. The model was applied to different systems described previously in the literature and the theoretical curves were compared with the available experimental data of three different betaines.
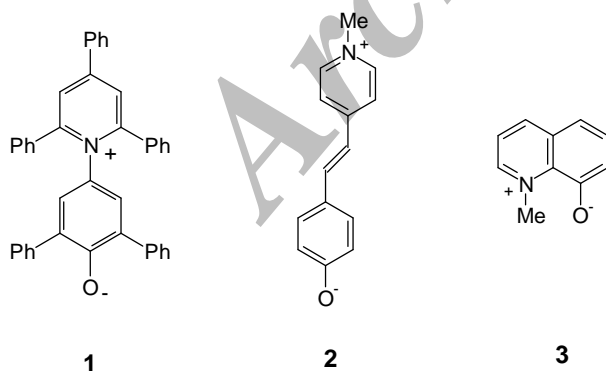
Scheme 1

Reichardt's $E_T(30)$ betaine (**1**), one of the most widely used solvatochromic probes [12], had its halochromic behaviour in alcoholic solutions described by us nearly twenty

years ago [6]. Merocyanine **2** has been the subject of investigation of various research groups [13,14] since it was first described by Brooker *et al*. [15,16]. Like dye **1**, it is a classic example of a dye that exhibits cationic halochromism [5]. The 1-methyl-8-oxyquinolinium dye **3** was originally described by Ueda and Schelly [17]. Its solvatochromic behaviour, recorded in a variety of solvents, correlates very closely with the corresponding $E_T(30)$ values [18]. Its halochromic behaviour in a variety of alcohols and non-protic solvents in the presence of sodium iodide, potassium and lithium perchlorate was also described by the authors [8].

CALCULATION METHODS

Molecular Dynamics Simulation Methods

40-Å solvent boxes of methanol and DMSO were built with the aid of Packmol [19], taking into account the solvent densities at 300 K. The structure of betaine **3** was generated by means of InsigthII [20], its geometry was optimised at the DFT level of theory with the hybrid functional B3LYP and the basis set 6-31G* and its atomic charges were corrected with the RESP protocol. Compound **3** was then inserted into the boxes with the aid of VMD [21] and molecular dynamics simulations of the system were carried out with NAMD [22] according to a protocol that started with an initial 250.000-step equilibration of the system at 0 K; the system temperature was then raised to 300 K in 1000 steps, followed by molecular dynamics simulation and an acquisition period of 2 ns.

Quantum Mechanics Calculations

Transition energies of all dyes polarized by a cation M^{n+} at a variable distance from their oxygen atom were obtained following the protocol described above. Firstly, the structures of compounds **1**, **2** and **3** were generated by means of InsightII [20] and their geometries were optimised with the DFT B3LYP/6-31G* method. A cation M^{n+} was then positioned at a fixed distance from the oxygen atom of the dye, colinearly with its C-O bond. The resulting structure was then optimised again, keeping the O-M distance constant, with the semi-empirical AM1 method, with the *ab initio* HF/6-31G*, or with the hybrid DFT B3LYP/6-31G* methods. This procedure was repeated for different O-M distances, so as to obtain optimised structures polarized by cations situated at various distances

from the oxygen atom. Different levels of theory were employed in these optimisations, to make sure that the smooth variations of the transition energies with the O-M distances did not depend on the employed method, being very similar to a semi-empirical, an HF or a hybrid DFT method. The Gaussian G98 package [23] was employed for these optimisations and subsequent energy-calculations. Transition energies were then obtained by single-point calculations on the optimised structures, employing the ZINDO/S method and configuration interactions involving singly-excited transitions among the 10 highest occupied and the 10 lowest unoccupied molecular orbitals of the molecules. Transition energies were also estimated with a TD-DFT method (B3LYP/6-31G*) and the results were compared with the CI-ZINDO/S method.

For calculations of the halochromic shifts in solution, Zerner's INDO/S program was employed [24]. Each dye-cation superstructure, optimised as described above, was subjected to a single-point calculation employing the SCRF-PCM option with dielectric constants of 20.7 and 36.6 for acetone and acetonitrile, respectively.

RESULTS AND DISCUSSION

Molecular Dynamics Simulations

Molecular dynamics simulations of solutions of the oxyquinolinium betaine **3** in the presence of an alkali cation (Na^+) were run for four different cation concentrations (0.1, 0.15, 0.20 and 0.25 M) in methanol, and in five different concentrations (0.1, 0.15, 0.20, 0.25 and 0.5 M) in DMSO. Information about the solvation shells in solution could be obtained from radial distributions of solvent molecules or of the sodium cations around the oxide substituent.

The authors had previously studied the solvation of four phenolate betaines in protic solvents (water, methanol and 2-propanol) and in DMSO [25]. The first solvation layer of the phenolate oxygen of **3** in methanol yielded a peak distance of 2.8 Å. This value was in good agreement with the value of 2.7 Å obtained by Mente and Maroncelli [26] for O-O distribution functions of the $E_T(30)$ phenolate oxygen in ethanol and other alcohols. A similar value had also been reported by Canuto *et al*. [27] for the O-O distribution function of the *ortho*-pyridinium phenolate betaine in water.

When Na^+ cations were incorporated into the methanolic

box with betaine **3**, the system evolved to cationic solvation layers around the oxygen atom of the dye, with peak distances that varied with the Na^+ concentration. Figure 1 reproduces the radial distribution function (RDF) of sodium cations around the oxygen atom of **3**, in a 0.2 M methanolic solution of Na^+. According to this graph, *ca*. 2.5 Na^+ cations comprise the first solvation layer, at a distance of 4.5 Å from the oxygen atom of **3**.

Figure 2 depicts the O-Na radial distribution of sodium cations in a DMSO solution of **3**, for the variable concentrations of Na^+. As can be seen, the sodium cations accumulate in solvation shells which get increasingly closer to the oxygen atom of **3**, as the bulk Na^+ concentration is increased.

The above results are summarized in Table 1, which lists the O-Na peak distances and the number of Na^+ cations present in each solvation shell, for all of the methanolic and DMSO solutions of **3**.

The data show that in both solvents, the microenvironment around the oxygen atom of **3** becomes gradually enriched in Na^+ cations, as the sodium bulk concentration is increased. In addition, the average distance between the sodium cations and the oxide atom is reduced with the increasing Na^+ concentration.

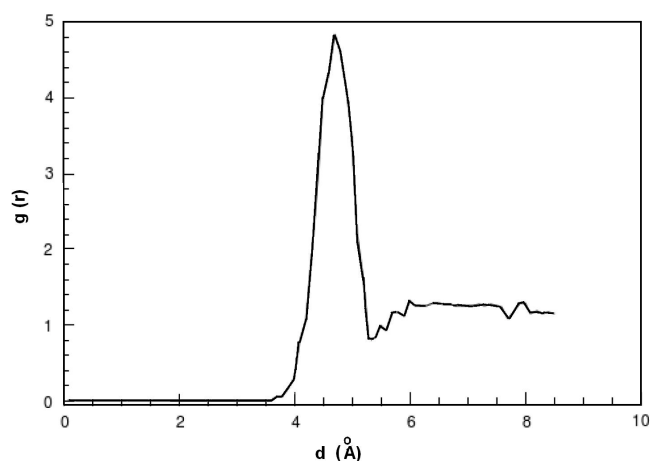Similarly, the halochromic behaviour of phenolate betaines

Fig. 1. O-Na radial distribution of sodium cations in a 0.2 M Na^+ methanolic solution of **3**.
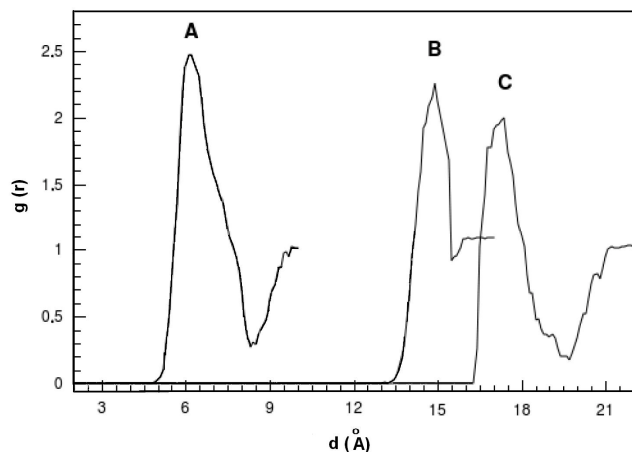
997

Fig. 2. O-Na radial distribution of sodium cations in DMSO solutions of **3** containing (a) 0.5, (b) 0.2 and (c) 0.1 M Na$^+$.

Table 1. O-Na Peak Distances r and Number N_{Na} of Na$^+$ Cations Present in the First Solvation Shell of the Oxygen Atom of **3**, in Methanol and DMSO

[Na$^+$] (M)	MeOH		DMSO	
	r (Å)	N_{Na+}	r (Å)	N_{Na+}
0.10	8.8	1.0	17.4	0.9
0.15	6.9	2.4	15.5	1.0
0.20	4.7	3.7	14.9	1.7
0.25	4.6	4.2	6.3	3.5
0.50	4.5	5.1	6.2	4.4

may be assumed to be arising from polarity variations of their environment, induced by cations distributed at a variable distance from the phenolate oxygen.

Theoretical Model

Based on the picture that emerged from the molecular dynamics simulations, we developed a model to estimate the effect of an approaching cation on the halochromic transition energy of a phenolate betaine.

Some simplifications were necessary for applying the results from the dynamics to the reproduction of an
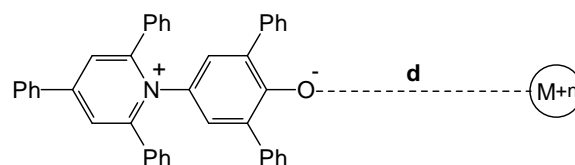
Scheme 2

experimental behaviour with the aid of quantum mechanics calculations. The first had to do with the choice of fixed spatial arrangements for our calculations. Rdf's are obtained as averages of a large number of frozen frames. The spatial distribution of sodium cations in the solvating shell of a given phenolate is averaged over their positions in all frames. On the other hand, quantum mechanics calculations must be performed on supermolecules with defined positions for all atoms. We had, therefore, to replace this average distribution of cations in space for one or more cations in a fixed spatial arrangement. The simplest way to do this was to nominate just one cation, at a variable distance from the phenolate oxygen of the dye. By recording the $S_0 \rightarrow S_1$ transition energy of the system for this supermolecule, as shown for molecule **1**, we arrived at same values which varied significantly with the O-M^{n+} distance.

This conformation proved superior to other arrangements, where the O-M axis formed a different angle with the C-O bond. Contrary to other conformations, where sparkles (positive charges) were positioned above and below the oxygen atom of dye **2,** with results that contradicted experimental observations [28], our supermolecular model reproduced experimental trends quite favourably.

Secondly, in order to compare results obtained from this supermolecular model with experimental plots of transition energies *vs*. cation concentrations [M^{n+}], these concentrations had to be expressed in terms of some model parameter, like, for example, the cation-oxygen distance *d*. Assuming an electrolyte concentration (10^{-3}-10^{-2} M) that was much larger than that of the betaine (*ca*. 10^{-4} M), we envisaged the cationic media as very large cubic reticulates with the vertices occupied by M^{n+}. A relatively small number of these cations are replaced by the charged oxygen atoms of the phenolate donor. In this purely geometric arrangement, for an average

998

cation-oxygen distance d, the number of cations present in a cubic volume V of side a was given by $N = a^3/d^3$ and the molar cation concentration by $[M^{n+}] = N/N_A = a^3/N_A \, d^{\,3}$, where N_A is the Avogadro number. This simple relationship helped us postulate that the cation concentration was proportional to d^{-3}, $[M^{n+}] \propto d^{-3}$, so that the variable d^{-3} could be employed in our theoretical plots as an equivalent of $[M^{n+}]$.

Calculation of Halochromic Shifts in the Gas Phase

In order to verify the consistency of our model, we employed semi-empirical (AM1) and *ab initio* methods (HF/6-31G*) for the optimisation of the dye-cation complex. Both methods had been employed before, in computer simulations of the solvatochromism of **1** [26]. The semi-empirical AM1 method had also been employed in theoretical studies on the spectroscopic properties of **2** [14,28]. The resulting optimised structures were then subjected to a CI ZINDO/S calculation, for the estimation of the $S_O \rightarrow S_1$ transition energies. In all cases, these transitions corresponded to internal charge-transfer processes from the donor phenolate oxygen to the acceptor pyridinium or quinolinium system, with a major contribution of the monoelectronic HOMO $\rightarrow$ LUMO excitation.

As shown below, in a few cases the optimisation method affected the absolute values of the obtained transition energies. In other cases, however, employing a semi-empirical or an *ab initio* method for the initial optimisation of the system led to practically the same excitation energies. As stated above, the theoretical excitation energies, being the result of gas-phase calculations, were not expected to match experimental values in solution.

We also employed a different approach for the calculation of the theoretical transition energies, employing a TD-DFT method. After optimizing the dye-cation complex structures with the hybrid B3LYP/6-31G* method, a TD calculation employing the B3LYP/6-31G* option was done. However, the obtained transition energies were unacceptably small, departing more drastically than the ZINDO/S results from the experimental values. Such a result was not unexpected. Failures of TD-DFT methods for the calculation of charge-transfer excitation energies in conjugated molecules are well documented [29].

Figure 3a depicts plots of the theoretical $S_0 \rightarrow S_1$ transition

energies of **1** against d^{-3}, where d is the distance between the cation M^{n+} and the phenolate oxygen of the dye. Optimisations of the dye-cation complex were performed with the AM1 and the HF/6-31G* methods for lithium, sodium and calcium. In all cases, the excitation energies obtained by the CI ZINDO/S option were practically the same for both semiempirical and *ab initio* optimisations.

The theoretical plots should be compared with the experimental data [6] shown in Fig. 3b, where $E_T(30)$ values of ethanolic solutions of betaine **1** containing increasing concentrations of sodium, lithium or calcium perchlorate are plotted against the concentration of the added cation. Association between the phenolate donor and the harder Ca^{2+} cation than that of Li^+ and Na^+, resulting in larger halochromic shifts in ethanolic solutions of the former. This effect is reproduced theoretically, according to our model. Similar comparisons between theoretical results and experimental data are shown in Figs. 4 and 5.

In all cases, theory tended to exaggerate the halochromic shifts caused by the proximity of a cation. This is a consequence of the fact that calculations ignored the effect of the solvent, which tends to shield the dye from the charged cation. Thus, for example, the comparison of Figs. 3a and 3b shows that, although the theoretical curves are qualitatively similar to the experimental ones, the predicted halochromic shifts, in the gas phase, are *ca.* three-fold larger than the observed shifts in ethanol.

In Fig. 4a we have plotted the $S_0 \rightarrow S_1$ transition energies of **2** against d^{-3}, where d is the distance between a sodium or a lithium cation and the phenolate oxygen of the dye. Optimisations were performed at a semiempirical (Na^+, AM1 method) or a semiempirical and *ab initio* level (Na^+, Li^+, AM1 and HF/6-31G* methods). In the latter case, the CI ZINDO/S excitation energies were practically the same, irrespective of the method employed for the optimisation. The experimental data [5] for the halochromic behaviour of merocyanine **2** in acetonitrile, in the presence of increasing concentrations of $LiClO_4$ and NaI, are shown in Fig. 4b. The theoretical curves are very similar to the experimental ones, although the predicted values of the halochromic shifts are considerably awayfrom the experimental shifts in acetonitrile.

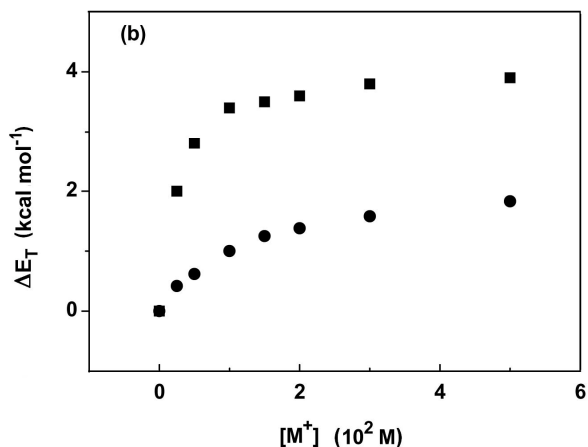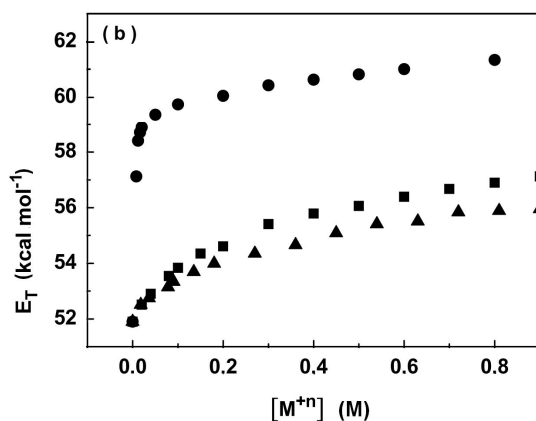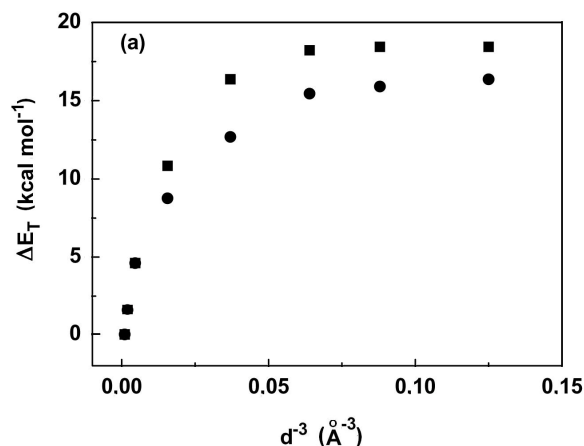In Fig. 5a, theoretical transition energies of oxyquinolinium **3** are plotted against our concentration
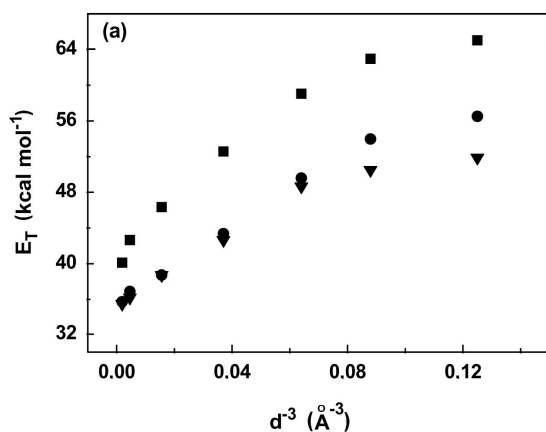
999

Fig. 3 (a) Variation of the theoretical $S_O \rightarrow S_1$ transition energy of **1**, calculated with the ZINDO/S method, in the presence of increasing concentrations of Li^+, Na^+ or Ca^{+2}. The cation concentrations are assumed proportional to d^{-3}, where d is the cation-oxygen phenolate distance (see text). Optimisations were performed at a semiempirical (Na^+ and Ca^{2+}, AM1 method), and an *ab initio* level (Ca^{2+}, HF/6-31G* method). Excitation energies in the presence of Ca^{2+} were practically the same for the semiempirical and the *ab initio* optimisations: (■) Ca^{2+}, (●) Na^+; (▼) Li^+, (b) Variation of the $E_T(30)$ values of ethanolic solutions of Reichardt's betaine **1** in the presence of increasing concentrations of $NaClO_4$, $LiClO_4$ or $Ca(ClO_4)_2$ (see Ref. [6]): (●) $Ca(ClO_4)_2$, (■) $LiClO_4$, (▲) $NaClO_4$.

Fig. 4. (a) Variation of the theoretical halochromic shift of **2** in the presence of increasing concentrations of Li^+ and Na^+, calculated with the ZINDO/S method. The cation concentration is assumed proportional to d^{-3}, where d is the cation-oxygen distance (see text). Optimisations were performed at a semiempirical (Na^+ and Li^+, AM1 method), and an *ab initio* level (Li^+, HF/6-31G* method). Excitation energies in the presence of Li^+ were practically the same for the semiempirical and the *ab initio* optimisations: (■) Li^+, (●) Na^+; (b) Variation of the halochromic shift of **2** in acetonitrile, in the presence of increasing concentrations of $LiClO_4$ or NaI (see Ref. [5]): (■) $LiClO_4$, (●) NaI.
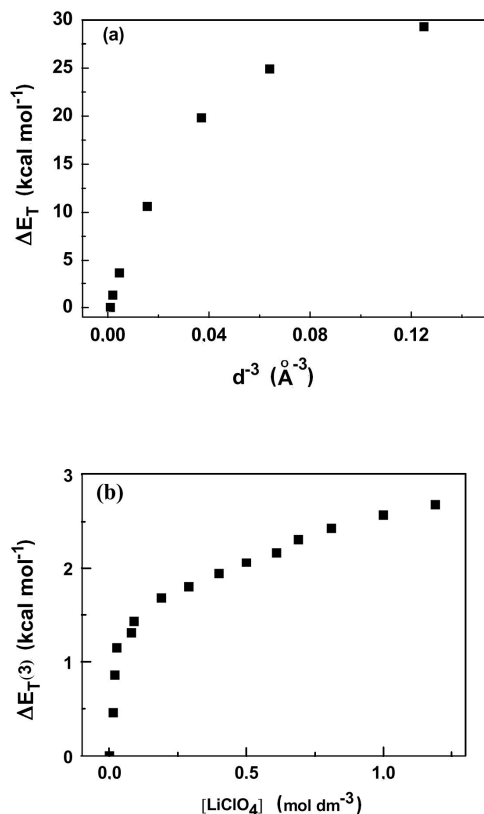
Fig. 5. (a) Variation of the theoretical halochromic shift of **3** in the presence of increasing concentrations of Li$^+$, calculated with the ZINDO/S method. The lithium concentration is assumed proportional to d^{-3}, where d is the cation-oxygen distance (see text). Optimisations were performed at the *ab-initio* HF/6-31G* level: ($\blacksquare$) Li$^+$; (b) Variation of the halochromic shift of **3** in 2-propanol, ΔE_T, in the presence of increasing concentrations of LiClO$_4$ (see Ref. [8]).

parameter d^3, where a Li$^+$ cation is brought gradually closer to the oxygen atom of this dye. Optimisations were performed with the AM1 and the HF/6-31G* methods. The latter method yielded the curve presented, for the corresponding ZINDO/S excitation energies. Although the *ab initio* optimisations yielded smaller excitation energies than the semiempirical AM1 method, both curves reproduced quite adequately the qualitative trends depicted in Fig. 5b, for the halochromic behaviour of **3** in 2-propanol, in the presence of LiClO$_4$ [8].
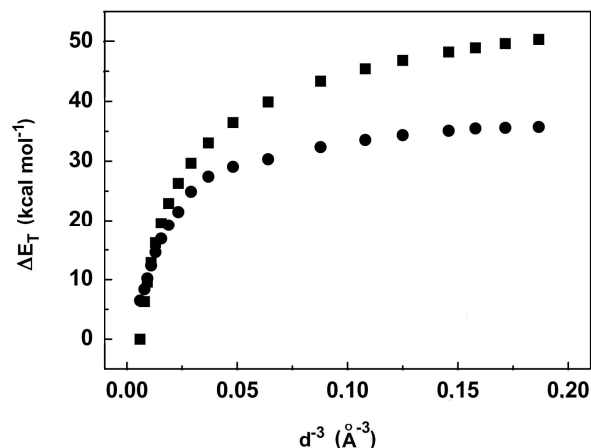

Fig. 6. Variation of the halochromic shift ΔE of **2**, in acetonitrile and acetone, in the presence of increasing concentrations of Li$^+$, calculated with the ZINDO/S method. The lithium concentration is assumed proportional to d^{-3}, where d is the cation-oxygen distance (see text).

The theoretical shift of *ca.* 30 kcal mol^{-1}, calculated in the gas phase, was 10-fold larger than the experimental one, recorded in 2-propanol.

Calculation of Halochromic Shifts in Solution

Halochromic shifts depend on the nature of the phenolate betaine, on the cationic species present in solution and on the solvent. The above results, obtained without the consideration of any solvent, agreed with the experimental observations wherein shifts increase with the cation hardness. Shifts also vary with the solvent, being larger in less polar media.

We investigated the effect of the solvent on the theoretical halochromism of betaine **2** by comparing its behaviour in the presence of increasing concentrations of Li$^+$ in acetonitrile (ε = 36.6) and acetone (ε = 20.7). This was carried out by calculating, for all previously optimised dye-cation pairs in the gas phase, the corresponding transition energies in a continuum, employing the SCRF-PCM option, and Zerner's INDO/S [24].

The results are shown in Fig. 6. As can be seen, the halochromic shifts were smaller in the more polar solvent

1001

(acetonitrile), in agreement with the experimental observations where dye-cation interactions are reduced in more polar media.

Although capable of discriminating between solvents of different dielectric constants, the PCM option still predicted halochromic shifts that were significantly larger than the experimental ones. This limitation of a continuum model that ignores specific solute-solvent interactions has been recognized by different authors, when trying to reproduce solvent effects on solvatochromic dyes [26,30,31].

CONCLUSIONS

In conclusion, simulations carried out on methanolic and DMSO solutions of a solvatochromic betaine, in the presence of increasing concentrations of Na^+, led to a picture for the solvation of the dye, based on radial distribution functions of solvent molecules, or sodium cations, around the anionic oxygen of the betaine. According to this picture, as the Na^+ concentration was increased, tighter, solvent-separated ion-pairs were formed in solution, where the average $O-Na^+$ distance was gradually reduced. Similarly, a simple model for the qualitative reproduction of the halochromic behaviour of phenolate dyes was developed, based on the calculation of the transition-energy of the longest-wavelength band of the dye in the presence of a cation positioned at a variable distance from its phenolate oxygen. A comparison of the obtained theoretical curves with the experimental data in the literature showed that the employed model, in spite of its simplicity and of all approximations involved, successfully mimicked the cationic halochromism of phenolate dyes. The calculated halochromic shifts depend on the phenolate betaine and on the interacting cation, increasing with their hardness in the order $Na^+ < Li^+ < Ca^{2+}$. Calculations employing a continuum model, to mimic dye-cation interactions in solution, were also congruent with the experimental observations where halochromic shifts were larger in a less polar solvent, like acetone, than in the more polar acetonitrile.

ACKNOWLEDGEMENTS

REFERENCES

[1] A.D. McNaught, A. Wilkinson, IUPAC Compendium of Chemical Terminology, 2nd ed., Blackwell Science, 1997.

[2] C. Reichardt, Chem. Soc. Rev. 21 (1992) 147.

[3] G. Laus, H. Schottenberger, K Wurst, J. Schütz, K.-H. Ongania, U.E. Horvath, Org. Biomol. Chem. 1 (2003) 1409.

[4] J.K. Basu, M. Shannigrahi, N. Ray, S. Bagchi Spectrochim. Acta A 61 (2005) 2539.

[5] S.P. Zanotto, M. Scremin, C. Machado, M.C. Rezende, J. Phys. Org. Chem. 6 (1993) 637.

[6] M.C. Rezende, Tetrahedron 44 (1988) 3513.

[7] C. Machado, M.G. Nascimento, M.C. Rezende, J. Chem. Soc. Perkin 2 (1994) 2539.

[8] V.G. Machado, M.G. Nascimento, M.C. Rezende, Spectrosc. Lett. 31 (1998) 359.

[9] V. Gageiro, M. Aillon, M.C. Rezende, J. Chem. Soc. Faraday Trans. 88 (1992) 201.

[10] D.A. Binder, M.M. Kreevoy, J. Phys. Chem. 98 (1994) 10008.

[11] D. Zanette, C. Zucco, M.C. Rezende, Tetrahedron 41 (1985) 87

[12] C. Reichardt, Solvents and Solvent Effects in Organic Chemistry, 3rd ed., Wiley-VCH, Weinheim, 2003.

[13] A. Botrel, A. Le Beuze, P. Jacques, H. Strub, J. Chem. Soc. Faraday Trans. 2, 80 (1984) 1235.

[14] J.O. Morley, R.M. Morley, R. Docherty, M.H. Charlton, J. Am. Chem. Soc. 119 (1997) 10192.

[15] L.G.S. Brooker, C.H. Keys, R.H. Sprague, R.H. Van Dyke, F. Van Zandt, F.L. White, H.W.J. Cressman, S.G. Dent, J. Am. Chem. Soc. 73 (1951) 5332.

[16] L.G.S. Brooker, C.H. Keys, D.W. Heseltine, J. Am. Chem. Soc. 73 (1951) 5350.

[17] M. Ueda, Z.A. Schelly, Langmuir 5 (1989) 1005.

[18] L.P. Novaki, O. El Seoud, Ber. Bunsenges. Phys. Chem. 100 (1996) 648.

[19] J.M. Martínez, L. Martínez, J. Comput. Chem. 24 (2003) 819.

[20] InsightII User Guide; Accelrys: San Diego, 1998.

[21] W. Humphrey, A. Dalke, K. Schulten, J. Mol. Graphics 14 (1996) 33.

[22]   J.C. Phillips, R. Braun, W. Wang, J. Gumbart, E. Tajkhorshid, E. Villa, C. Chipot, R.D. Skeel, L. Kale, K. Schulten, J. Comput. Chem. 26 (2005) 1781.

[23]   Gaussian 98, Revision A.11.3, M.J. Frisch, G.W. Trucks, H.B. Schlegel, G.E. Scuseria, M.A. Robb, J.R. Cheeseman, V.G. Zakrzewski, J.A. Montgomery, Jr., R.E. Stratmann, J.C. Burant, S. Dapprich, J.M. Millam, A.D. Daniels, K.N. Kudin, M.C. Strain, O. Farkas, J. Tomasi, V. Barone, M. Cossi, R. Cammi, B. Mennucci, C. Pomelli, C. Adamo, S. Clifford, J. Ochterski, G.A. Petersson, P.Y. Ayala, Q. Cui, K. Morokuma, N. Rega, P. Salvador, J.J. Dannenberg, D.K. Malick, A.D. Rabuck, K. Raghavachari, J.B. Foresman, J. Cioslowski, J.V. Ortiz, A.G. Baboul, B.B. Stefanov, G. Liu, A. Liashenko, P. Piskorz, I. Komaromi, R. Gomperts, R.L. Martin, D.J. Fox, T. Keith, M.A. Al-Laham, C.Y. Peng, A. Nanayakkara, M. Challacombe, P.M.W. Gill, B. Johnson, W. Chen, M.W. Wong, J.L. Andres, C. Gonzalez, M. Head-Gordon, E.S. Replogle,

J.A. Pople, Gaussian, Inc., Pittsburgh PA, 2002.

[24]   ZINDO: A Semi-Empirical Program Package, M.C. Zerner, University of Florida, Gainesville, FL 32611, USA.

[25]   C. Mascayano, M.C. Rezende, C. Mendez, G. Núñez, V. Chiang, J. Sol. Chem. 38 (2009) 363.

[26]   S.R. Mente, M. Maroncelli, J. Phys. Chem. 103 (1999) 7704.

[27]   M.Z. Hernandez, R. Longo, K. Coutinho, S. Canuto, Phys. Chem. Chem. Phys. 6 (2004) 2088.

[28]   J.O. Morley, J. Mol. Struct. (Theochem.) 301 (1994) 191.

[29]   A. Dreuw, M. Head-Gordon, Chem. Rev. 105 (2005) 4009.

[30]   M. Beckett, J. Dawber, J. Chem. Soc. Faraday Trans. 1 85 (1989) 727.

[31]   R.B.de Alencastro, J.D.D.M. Neto, M.C. Zerner, Int. J. Quantum Chem. Quantum Chem. Symp. 28 (1994) 361.